

1 Missing atmospheric noble gases in a large, tropical lake: 2 the case of Lake Kivu, East-Africa

3

4 Fabian Bärenbold^{1*}, Martin Schmid¹, Matthias S. Brennwald² and Rolf Kipfer^{2,3}

5

6 ¹ Eawag, Swiss Federal Institute of Aquatic Science and Technology, Surface Waters - Research
7 and Management, Kastanienbaum, Switzerland

8 ² Eawag, Swiss Federal Institute of Aquatic Science and Technology, Water Resources and
9 Drinking Water, Dübendorf, Switzerland

10 ³ ETH Zurich, Inst. of Biogeochemistry and Pollution Dynamics & Inst. of Geochemistry and Petrology,
11 Zürich, Switzerland

12

13

14 *Corresponding author, e-mail: fabian.baerenbold@eawag.ch

15

16 **Abstract**

17 *Lake Kivu is a 485 m deep tropical rift lake in East-Africa and well-known for its very high*
18 *concentrations of dissolved carbon dioxide and methane in the stratified deep waters. In view of*
19 *future large-scale methane extraction for power production, there is a need for predicting the*
20 *evolution of gas concentrations and lake stability using numerical modelling. However, knowledge*
21 *about the geochemical origin and transport processes affecting dissolved gases in the lake is still*
22 *partially missing. Due to their inert nature, the analysis of dissolved noble gases can help to shed*
23 *light on such questions. To learn more about transport processes in Lake Kivu, we extended a well-*
24 *established sampling method for dissolved noble gases to work in the lake's high gas pressure*
25 *waters. The results of our analysis show a distinct non-atmospheric isotopic signal in the deep*
26 *waters (below 250 m) with ³He/⁴He and ⁴⁰Ar/³⁶Ar ratios ~250% and ~20% higher than air*
27 *saturated water (ASW). Moreover, the gas concentration profiles reveal a striking lack of*
28 *atmospheric noble gases in the deep waters with respect to ASW. While Ne is depleted by ~45%,*
29 *the more soluble ³⁶Ar and Kr even decrease by ~70%. In contrast, ⁴He concentrations increase*

30 *with depth by a factor of up to ~600. We attribute this excess He and the increases in $^3\text{He}/^4\text{He}$ and*
31 *$^{40}\text{Ar}/^{36}\text{Ar}$ to the inflow of magmatic gases into Lake Kivu, along with a significant contribution of*
32 *radiogenic ^4He . To explain the depletion of atmospheric noble gases, we present and discuss three*
33 *different scenarios, namely continuous outgassing, the inflow of depleted groundwater and a large*
34 *past outgassing event. Due to the best agreement with our observations, we conclude that the inflow*
35 *of depleted groundwater is likely responsible for the observed atmospheric noble gas depletions.*

36 Keywords: noble gases; Lake Kivu; depletion; groundwater; volcanic region

37 **1 Introduction**

38 Meromictic Lake Kivu is part of the East African rift system and is located on the border between Rwanda
39 and the Democratic Republic of the Congo. It has a surface area of 2386 km² and a maximum depth of 485
40 m. The rather small catchment area of around 5100 km² (excluding lake area) includes part of the Virunga
41 volcano chain to the North of the lake. In this northernmost part of the catchment, there is no surface runoff
42 (Figure 1), but the rainfall feeds several subaquatic groundwater sources, which provide around 45 % of the
43 total inflow into the lake (1). Due to high salinity and carbon dioxide (CO₂) content, some of these sources
44 stratify close to the lake bottom, while two large, less dense sources remain at ~180 and ~250 m (2,3).
45 Consequently, steep physical and chemical gradients can be observed at these depths due to the dilution of
46 upwelling deep water rich in nutrients, gases and salts (4). This situation leads to a strong density
47 stratification, which suppresses turbulent mixing and therefore attenuates the upward transport of gases and
48 nutrients (2). In fact, the stratification effectively prevents annual mixing below a depth of around 50 – 65
49 m and thus enables the accumulation of CO₂ and biologically produced methane (CH₄) (5,6) over hundreds
50 of years in the vertically stratified and horizontally mixed deep waters.

51 On one hand, the high CH₄ concentrations of up to 20 mmol/L (2) represent a valuable resource, which is
52 commercially exploited for electricity production by a 26 MW power plant since December 2015. On the
53 other hand, the high total dissolved gas pressure (TDGP) in Lake Kivu is also a looming danger with a

54 possible gas eruption endangering the life of around 2 million people around the lake. Indeed, the analysis
55 of sediment cores in Lake Kivu indicates that mixing events have taken place in the past (7) and that the
56 most recent (partial) mixing event may have happened about 1000 years ago (8).

57 In view of future large-scale gas extraction and changing lake temperatures (9), it is important to predict
58 the lake's response to such changes. A one-dimensional model has been used in the past to understand gas
59 and nutrient dynamics (2) and to predict the effect of gas extraction on stratification stability, nutrients and
60 gas concentrations (10). Since the development of this model, detailed investigations allowed better
61 constraining the nutrient and methane cycles in the lake (4,6). Furthermore, some of the subaquatic
62 groundwater sources were located in the lake by Ross et al., (3). Nevertheless, there still persists a gap of
63 knowledge regarding transport processes within Lake Kivu as well as the origin and gas content of the
64 groundwater inflows.

65 The chemically and biologically inert noble gases can provide valuable insight into gas and water
66 dynamics of water bodies (see review by Kipfer et al., (11)). In particular, noble gas profiles could help

67 constraining turbulent mixing in Lake Kivu or reveal potential outgassing processes (11,12). In addition,
68 noble gas isotopic ratios can give hints about the origin of inflowing magmatic gases or fluids (13).

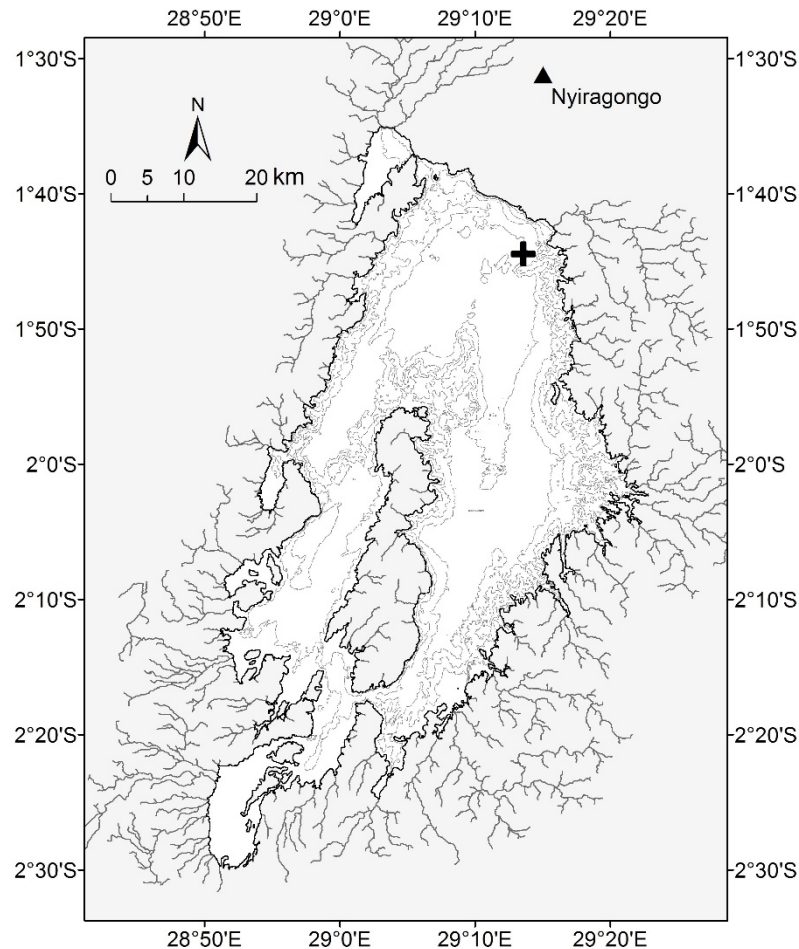


Figure 1: Lake Kivu bathymetry with contour lines every 100 m and surface tributaries. The cross indicates the sampling site (1.74087°S/29.22602°E) with a depth of 413 m. The triangle represents the active Nyiragongo volcano. Note the absence of surface run-offs in the northernmost region due to infiltration into the porous volcanic rock.

69
70 In this work, we present an extensive dataset of noble gas concentrations from two field campaigns which
71 took place at the northern shore of the Rwandan part of Lake Kivu. We start by describing the specially
72 designed sampling equipment for the high gas pressure conditions in Lake Kivu. Thereafter, we present
73 and discuss the recorded noble gas concentrations and isotope ratios in detail. In particular, we evaluate
74 three different scenarios to explain the observed depletion of atmospheric noble gases in the deep waters.

76 **2 Materials and Methods**

77 2.1 Sampling site and time

78 Water sampling was performed on the research platform of the LKMP (Lake Kivu Monitoring
79 Programme) 5 km off-shore in the northern part of the lake (Figure 1), From there, a maximum sampling
80 depth of around 410 m could be reached. An additional sample was taken from a boat 7 km further off-
81 shore at a depth of 440 m. We took 6 samples in January 2017 between 0 and 200 m and 11 samples in
82 March 2018 between 100 and 440 m.

83 Horizontal mixing dominates vertical mixing in Lake Kivu due to negligible vertical turbulent diffusion
84 (2) and a very slow upwelling (< 1 m/year, (4)) and thus, the lake can be assumed to be horizontally mixed
85 below 65 m. The high horizontal homogeneity is documented by well-matching vertical conductivity and
86 temperature profiles in different parts of the lake (3). Therefore, we can group together the samples from
87 different locations and years and merge them into one depth profile.

88 2.2. Description of sampling method and analysis

89 Dissolved gas sampling is challenging in water bodies where TDGP exceeds atmospheric pressure (in
90 Lake Kivu TDGP > 15 bar in the stratified deep waters). When the oversaturated water is lifted to the
91 surface, the lack of hydrostatic pressure typically leads to severe loss of dissolved gases. To overcome this
92 degassing of samples, we modified an existing in-situ sampling technique. As a starting point, we used the
93 standard noble gas sampling technique described in (14): copper tubes are flushed and filled with ~ 45 g of
94 sampling water, sealed gas-tight using the clamps of a metal rack and later degassed and analyzed in the
95 laboratory using mass spectrometry. In lakes without excessive gas content, the water is usually sampled
96 using a standard Niskin sampling bottle, retrieved and filled into the copper tube at atmospheric pressure.
97 The absence of atmospheric contamination is ensured by continuous flushing of the copper tube prior to
98 closing it.

99 This sampling method was first extended to outgassing lakes by Winckler et al. (15). They developed a
100 special in-situ sealing mechanism (see Figure 2 in (15)), using tapered metal plugs, which are pressed on
101 the copper tube ends by the force of large springs. To keep the copper tube open, the springs are
102 compressed by tripping levers which are attached to the triggering mechanism of a standard Niskin bottle
103 by a thin steel cable. In the field, the whole setup is lowered to the required depth and a falling weight is
104 used to release the springs and therefore close the copper tube. Back at the surface, the sample is
105 permanently sealed using the metal clamps. We applied this method in January 2017, but observed gas
106 loss in the samples below 200 m, and thus concluded that the springs were not strong enough to prevent
107 gas loss above a certain TDGP.

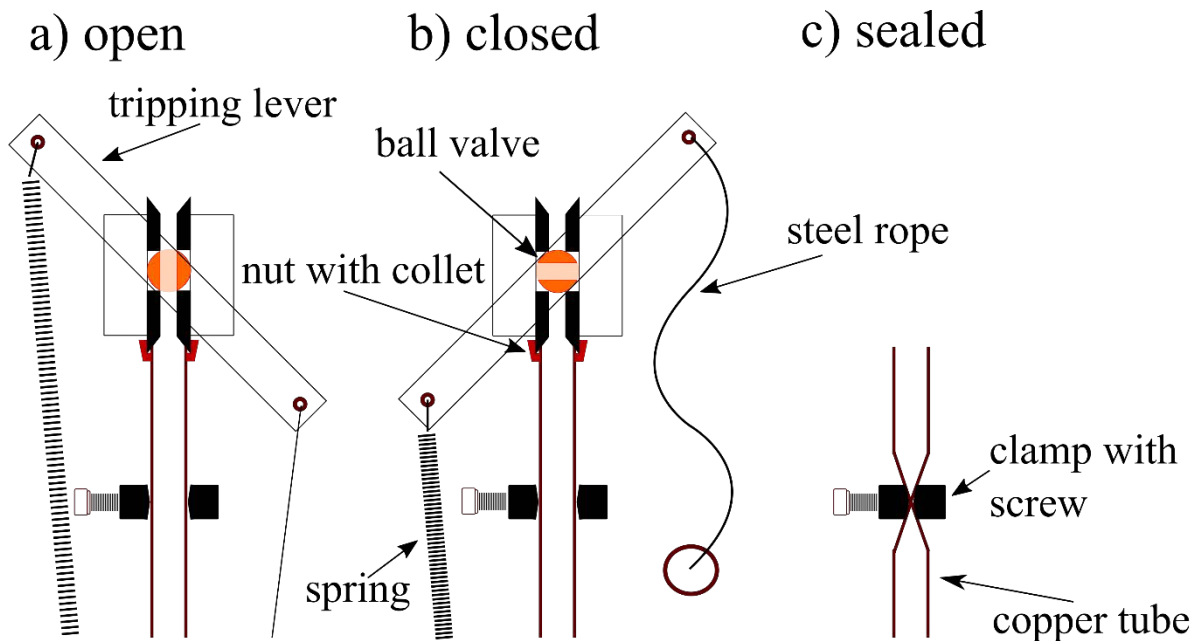


Figure 2: Schematic view and photo of the novel in-situ sealing mechanism using spring-loaded ball valves (Swagelok, pressure-proof to 172 bar). a) the tensioned steel rope keeps the ball valve open; b) the steel rope is detached (by a falling weight) and the spring closes the ball valve; c) the sample is permanently sealed using a metal clamp; d) photo of deployed sampling mechanism including a Niskin bottle (to use its trigger mechanism) and a buoy to keep the device upright in the water.

114 Therefore, we developed a new in-situ sealing-mechanism using pressure-proof Swagelok ball valves
115 (gastight up to 172 bar according to the manufacturer) instead of plugs (Figure 2). The valves are attached
116 on each side of the copper tube using vacuum seals and preloaded using metal springs (Figure 2a). At the
117 required sampling depth, the ball valves are triggered by a falling weight which closes the ball valves by
118 detaching the steel ropes (Figure 2b). Once retrieved, the samples are sealed permanently using the clamps
119 of the metal rack (Figure 2c). Finally, the samples are analyzed for noble gases ^4He , ^{20}Ne , ^{40}Ar , ^{86}Kr and
120 ^{136}Xe as well as isotope ratios $^3\text{He}/^4\text{He}$, $^{20}\text{Ne}/^{22}\text{Ne}$ and $^{40}\text{Ar}/^{36}\text{Ar}$ at the Noble Gas Laboratory at ETH
121 Zurich, Switzerland (14). Note that in the following sections, we usually give the total elemental
122 concentrations (computed from the isotopes) if not mentioned otherwise. The analytical uncertainty (1σ)
123 for gas concentrations and $^3\text{He}/^4\text{He}$ was determined to be between 0.5 and 1%, whereas for $^{20}\text{Ne}/^{22}\text{Ne}$ and
124 $^{40}\text{Ar}/^{36}\text{Ar}$ it was found to be around 0.2% (14). For this work, we chose to specify the uncertainty at the
125 3σ level (i.e. a 99.7% probability that the true value lies within the error margins). However, due to the
126 special gas composition in Lake Kivu samples with high amounts of CH_4 and CO_2 , these uncertainties are
127 estimated slightly higher at 5% (instead of 3%) for gas concentrations as well as $^3\text{He}/^4\text{He}$, and 1 %
128 (instead of 0.6%) for $^{20}\text{Ne}/^{22}\text{Ne}$ and $^{40}\text{Ar}/^{36}\text{Ar}$.

129 **3 Results**

130 **3.1 Noble gas concentrations**

131 The elemental noble gases Ne, Kr and Xe, as well as the isotope ^{36}Ar are called atmospheric noble gases
132 in the following because these elements/isotopes are predominantly of atmospheric origin in the
133 environment (11). The observed concentrations of these gases are presented in Tables 1 and 2, and Figure
134 3 shows the depth profiles of Ne, ^{36}Ar and Kr, normalized to the concentration of air saturated water
135 (ASW) at 25 °C and salinity of 0‰ (ASW calculated according to Weiss (16), Weiss (17) and Weiss and
136 Kyser (18)).

137 In the top 100 m, the concentrations of Ne, ^{36}Ar and Kr are approximately constant and close to ASW at
138 25 °C and 0 ‰ S (~5 % lower). Below, the concentrations consistently decrease with depth. This decrease

139 is probably linked to the inflows of subaquatic groundwater sources which were previously postulated and
 140 observed by (2) and (3), as summarized in Table 3. Between ~100 and 200 m, a gradual decrease is
 141 observed, in line with a diffuse groundwater source between 135 and 180 m (3). The largest concentration
 142 gradient is observed at ~250 m where a strong, fresh groundwater point source enters the lake and dilutes
 143 the upwelling deep water, which is rich in nutrients and dissolved gases (2,4). Below ~265 m, we observe
 144 a depletion of ~45% of Ne and even ~70% of the more soluble ³⁶Ar and Kr with respect to ASW. Note
 145 that although the salinity in Lake Kivu is rather high, this only results in a change in noble gas solubility
 146 (i.e. the Henry coefficient) of around 3 – 4% and therefore, cannot explain the observed noble gas
 147 depletions of ~45 and ~70% respectively.

148 **Table 1: Measured noble gas concentrations (in ccSTP/g) and isotope ratios. Air saturated water (ASW) concentrations**
 149 **are calculated according to (16,17,18) assuming a temperature of 25 °C and a salinity of 0‰. Note that we cannot explain**
 150 **the Xe concentrations and that they are not further discussed in this work.**

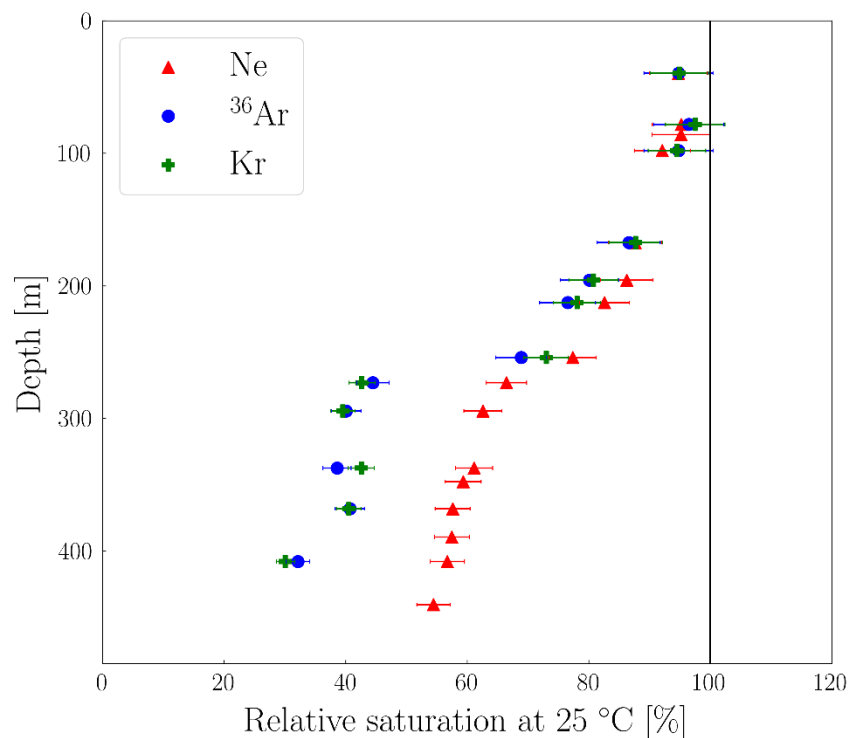
Depth [m]	³ He/ ⁴ He	He	²⁰ Ne/ ²² Ne	Ne	⁴⁰ Ar/ ³⁶ Ar	Ar	Kr	Xe
40	3.23E-06	7.19E-08	9.78	1.47E-07	296.1	2.34E-04	5.10E-08	6.89E-09
78	3.06E-06	1.90E-06	9.78	1.47E-07	297.4	2.40E-04	5.24E-08	7.07E-09
86	3.11E-06	2.61E-06	9.78	1.47E-07	298.3			
98	2.99E-06	3.92E-06	9.80	1.43E-07	298.8	2.36E-04	5.08E-08	7.29E-09
137	3.05E-06	6.20E-06	9.78					
167	3.31E-06	7.05E-06	9.78	1.36E-07	302.8	2.19E-04	4.71E-08	7.78E-09
196	3.13E-06	8.60E-06	9.79	1.34E-07	303.9	2.03E-04	4.34E-08	7.53E-09
213	3.29E-06	1.04E-05	9.78	1.28E-07	307.4	1.96E-04	4.19E-08	8.87E-09
254	3.68E-06	1.13E-05	9.78	1.20E-07	313.9	1.81E-04	3.92E-08	7.81E-09
273	4.41E-06	1.91E-05	9.79	1.03E-07	327.6	1.22E-04	2.29E-08	5.12E-09
294	4.16E-06	1.97E-05	9.80	9.69E-08	330.5	1.11E-04	2.13E-08	5.59E-09
337	4.33E-06	2.14E-05	9.81	9.47E-08	344.0	1.11E-04	2.29E-08	7.64E-09
348	4.72E-06	2.48E-05	9.80	9.18E-08	348.7			
368	4.79E-06	2.35E-05	9.77	8.92E-08	347.4	1.18E-04	2.18E-08	8.61E-09
390	4.57E-06		9.78	8.90E-08	352.9			
408	5.03E-06	2.38E-05	9.83	8.78E-08	350.6	9.41E-05	1.62E-08	8.05E-09
440	4.80E-06		9.81	8.43E-08	363.6			
Uncertainty	5 %	5 %	1 %	5 %	1 %	5 %	5 %	5 %
ASW	1.36E-06	3.83E-08	9.78	1.55E-07	295.5	2.46E-04	5.37E-08	7.41E-09

152 **Table 2: Noble gas concentrations (in ccSTP/g) and isotope ratios calculated from Table 1 (CO₂ and CH₄ data from M.**
 153 **Halbwachs and J.-C. Tochon in (2))**

Depth [m]	³ He	R/R _{air}	³⁶ Ar	⁴⁰ Ar*	³ He/ ⁴⁰ Ar*	⁴ He/ ⁴⁰ Ar*	CO ₂ / ³ He [x10 ⁹]	CH ₄ / ³ He [x10 ⁹]
40	2.32E-13	2.38	7.91E-07					
78	5.83E-12	2.25	8.05E-07					
86	8.11E-12	2.29						
98	1.17E-11	2.20	7.91E-07					
137	1.89E-11	2.24						
167	2.33E-11	2.43	7.23E-07					
196	2.69E-11	2.30	6.69E-07					
213	3.43E-11	2.42	6.39E-07					
254	4.15E-11	2.70	5.75E-07	1.06E-05	3.92E-06	1.07		
273	8.44E-11	3.24	3.71E-07	1.19E-05	7.08E-06	1.60	18.0	4.0
294	8.20E-11	3.06	3.35E-07	1.17E-05	6.99E-06	1.68	19.1	4.2
337	9.27E-11	3.18	3.22E-07	1.56E-05	5.93E-06	1.37	21.4	4.5
348	1.17E-10	3.47					17.2	3.6
368	1.12E-10	3.52	3.40E-07	1.77E-05	6.37E-06	1.33	17.9	3.7
390		3.36						
408	1.20E-10	3.69	2.69E-07	1.48E-05	8.09E-06	1.61	17.6	3.5
440		3.53						

154

155 Conversely, the Xe profile (not plotted in Figure 3) is devoid of any significant vertical structure, but
 156 exhibits a large variability. This is surprising as we are not aware of any process which would influence
 157 Xe fundamentally differently from Ne, ³⁶Ar and Kr in Lake Kivu. We thoroughly checked the data, but we
 158 found that samples from different lakes measured in the same measurement batch did not show any
 159 unusual behavior of Xe. In addition, the Lake Kivu Xe measurements are consistent over two different
 160 sampling campaigns and measurement batches in two different years. As we don't find any reason to
 161 discard the data, but cannot offer any explanation for this peculiar behavior of Xe in Lake Kivu we report
 162 the data in Table 1, but we do not further discuss it.



163

164 **Figure 3: Depth profiles of noble gas concentrations Ne, ³⁶Ar and Kr measured in January 2017 and March 2018.**
 165 Concentrations are normalized to the respective concentration of air saturated water at 25 °C and 0‰ S. ASW would be 3
 166 to 4% smaller if S = 6‰ was used instead (maximum value in Lake Kivu, see Figure 4). ³⁶Ar is calculated from ⁴⁰Ar
 167 concentration and ⁴⁰Ar/³⁶Ar ratio measurements.

168

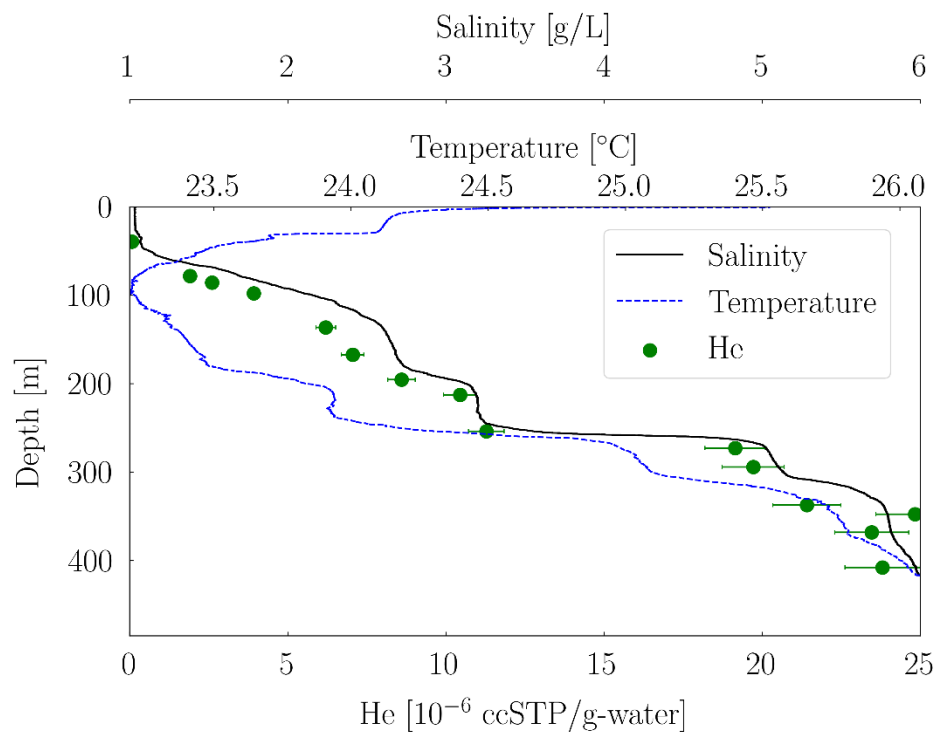
169 **Table 3: Depths, discharges, temperature and salinity of groundwater sources according to (2) and (3), who used a 1D lake**
 170 **model to estimate the sources and their properties. The groundwater sources 1 and 2 are called “fresh”, while the warmer,**
 171 **saltier sources 3-6 are called “hydrothermal” in this work. For the latter, the noble gas saturation depends on which**
 172 **scenario is chosen to explain the atmospheric noble gas depletion patterns (see discussion section).**

No.	Depth [m]	Discharge [m ³ /s]	Temp. [°C]	Salinity [g/L]	Atm. noble gas conc.
1	135 - 180	22	22.7 – 23.2	2.1 – 2.5	Close to ASW
2	250 - 255	15	23.3	2.7 – 3.1	Close to ASW
Total fresh		37			
3	315	1	25.2	3.4	Depleted?
4	365	1.5	24.5	5.5	Depleted?
5	425	0.8	25.3	5.8	Depleted?
6	465	1.25	26.0	6.0	Depleted?
Total hydrothermal		4.55			

173

174 In contrast to the atmospheric noble gases, He concentrations show a strong increase with depth by a
 175 factor of up to ~600 compared to ASW in Lake Kivu (Table 1 and Figure 4). Such high He concentrations

176 are commonly observed in lakes in volcanic environments and, according to Kipfer et al., (11) can be
177 ascribed to input of gases originating from the earth's mantle and/or radiogenic production within the
178 crust. Figure 4 also shows that the He concentrations correlate very well with salinity.
179 Depleted noble gas concentrations have already been observed in crater lakes Nyos and Monoun in
180 Cameroon, but with much higher variability (19). These lakes are much smaller than Lake Kivu but both
181 also have a history of gas eruptions (21,22) and are also located close to a volcanically active region. The
182 ^{20}Ne , ^{36}Ar and ^{84}Kr concentrations measured in these lakes are similar to our results in Lake Kivu (60 –
183 70% depletion in Nyos and 70 – 80% depletion in Monoun). However, unfortunately Nagao et al. (19) did
184 not further discuss this unusual depletion of atmospheric noble gases.



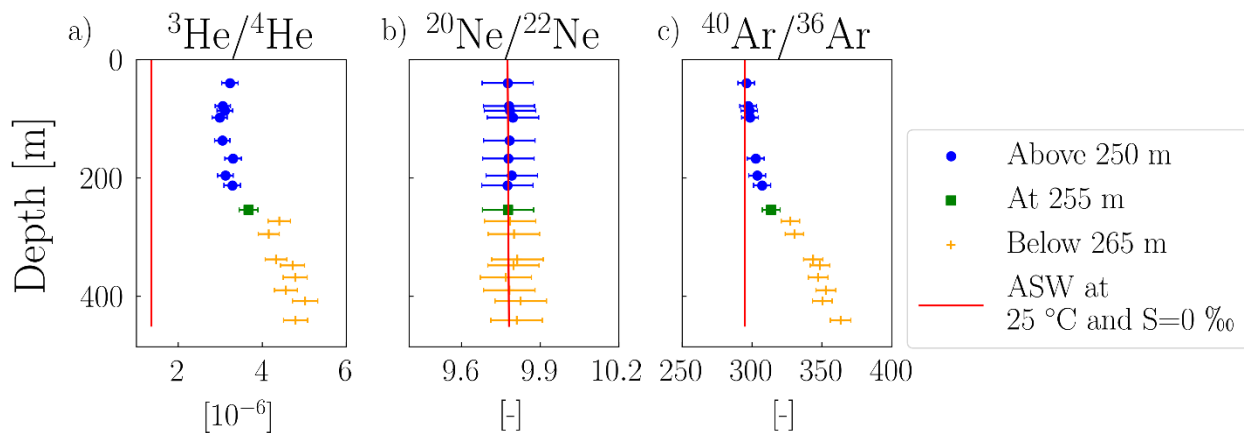
185 **Figure 4: The depth profile of Helium is shown along with salinity and temperature. ASW for He at 25 °C and 0‰ S is 0.038×10^{-6} ccSTP/g. Conductivity and temperature were recorded using a conductivity-temperature-depth profiler (CTD) from Sea & Sun in 2017 and 2018 (F. Bärenbold, unpubl.). Salinity is derived from conductivity using ionic composition according to (20). In Lake Kivu, salinity is mainly responsible for the density stratification.**

186

187

188 3.2 Noble gas ratios

189 The noble gas ratios $^3\text{He}/^4\text{He}$ and $^{40}\text{Ar}/^{36}\text{Ar}$ increase by around 60 and 20 % respectively from the lake
 190 surface to the bottom layer (Figures 5a and c; Table 1). At the surface, the $^{40}\text{Ar}/^{36}\text{Ar}$ ratio is close to air
 191 saturated water (ASW) and starts to slightly increase below 100 m. Between 200 and 300 m, the increase
 192 is more marked, but not as steep as the salinity and He gradients in Figure 4. In contrast to $^{40}\text{Ar}/^{36}\text{Ar}$, the
 193 $^3\text{He}/^4\text{He}$ ratio is still around 2.5 times above ASW at the lake surface, but exhibits a similar decrease
 194 below ~200 m. A very different behavior can be seen for the $^{20}\text{Ne}/^{22}\text{Ne}$ ratio (Figure 5b) which remains
 195 perfectly constant from 0 to 440 m. The maximum $^{40}\text{Ar}/^{36}\text{Ar}$ ratio of ~ 365 found in the Lake Kivu deep
 196 waters is roughly similar to the maximum value of 350 observed for fumaroles of the nearby Nyiragongo
 197 volcano, whereas it is around half for $^3\text{He}/^4\text{He}$ (~5 x 10⁻⁶ in Lake Kivu, ~11 x 10⁻⁶ in the fumaroles)(13).



198

199 **Figure 5: Depth profiles of measured isotopic ratios $^3\text{He}/^4\text{He}$, $^{20}\text{Ne}/^{22}\text{Ne}$ and $^{40}\text{Ar}/^{36}\text{Ar}$. The ratios in air saturated water**
 200 **(ASW) are shown for comparison.**

201

202 **4 Discussion**

203 4.1 Why are the atmospheric noble gases depleted?

204 As noble gases are inert, only physical gas processes can be responsible for any deviation of the measured
 205 concentrations from ASW at the respective temperature and salinity. In Lake Kivu (but also in Lakes Nyos

206 and Monoun), the depletion could be caused by 1) continuous outgassing either due to bubbles released
207 from the sediment or from a point source, 2) the inflow of hydrothermal water which is itself depleted
208 with respect to ASW or 3) a relic from a past, large outgassing event. In the following, we will evaluate
209 the consistency of each of the three scenarios with regard to our observations.

210 4.1.1 Scenario 1: Continuous deep water outgassing

211 Scenario 1 implies stripping of noble gases out of the deep water by gas bubbles containing mostly CH₄
212 and CO₂. Such bubbles could either originate from point sources (e.g. bubble seeps at the bottom, see for
213 example (12)) or from homogeneous ebullition at the sediment interface (23). However, Lake Kivu is very
214 deep and although its total dissolved gas pressure (TDGP) is very high, it is still significantly below
215 hydrostatic pressure (a maximum of around 50% is reached at 320 m, F. Baerenbold unpubl.). Therefore,
216 bubbles tend to redissolve at any depth. If the bubbles were produced by point sources, they would have to
217 travel all the way up to the mixed zone (above 50 m). Otherwise, we would observe an accumulation of
218 noble gases at some depths due to redissolution of bubbles. The existence of such accumulations is not
219 supported by our data, which show a monotonous decrease with depth.

220 The bubble dissolution model used in (24) predicts that bubbles would need to have a diameter larger than
221 around 20 mm in order to reach the mixed layer from the deepest point of Lake Kivu. This diameter is
222 much larger than bubble sizes observed for deep seeps (25,26). It therefore seems unlikely that gas
223 bubbles generated in the deep water can reach the lake surface. Conversely, if the gas bubbles were
224 created homogeneously at the lake-sediment interface, they would not necessarily need to reach the
225 surface to generate a net upwards transport of noble gases. In fact, bubbles could simply be generated at
226 the sediment interface, migrate upwards a certain distance and redissolve. Due to the fact that there is a
227 continuous lake-sediment interface at all depths, the result of such homogenous outgassing would be a
228 depletion of noble gases in the deep waters.

229 Although there are no observations of major continuous outgassing in Lake Kivu, there is some indication
230 of a free gas phase in the sediment (Figure 6 in (8)) and even a possible gas emanating structure (Figure 4a
231 in (27)). Potentially, larger noble gas stripping gas bubbles could originate from such free gas phases or
232 gas emanating structures.

233 In addition to a depletion of atmospheric noble gas concentrations, continuous outgassing should also alter
234 noble gas isotope ratios in the deep water by means of isotope fractionation at the bubble interface. The
235 reason for this is the difference in molecular diffusion between the isotopes. This process is explained in
236 detail in (28), and we can use Equation (1) in (28) to check whether our measured $^{20}\text{Ne}/^{22}\text{Ne}$ and $^{40}\text{Ar}/^{36}\text{Ar}$
237 ratios agree with a Rayleigh fractionation pattern. For this purpose, we use the Ne and Ar diffusion
238 coefficients found by (29) and our Ne and ^{36}Ar concentrations at the deepest sampling depth. The results
239 of this calculation indicate a $^{40}\text{Ar}/^{36}\text{Ar}$ ratio of ~ 315 for an Ar depletion of $\sim 70\%$ for the deepest sample of
240 this work. This means that only around 30 % of the observed increase of $^{40}\text{Ar}/^{36}\text{Ar}$ (up to ~ 365 , Figure 5c)
241 compared to ASW can be explained by bubble stripping. Furthermore, a $^{20}\text{Ne}/^{22}\text{Ne}$ ratio of around 9.72 is
242 predicted for the deepest sample if bubble stripping were responsible for the Ne depletion of $\sim 45\%$ in
243 Lake Kivu. However, we observe a constant $^{20}\text{Ne}/^{22}\text{Ne}$ ratio of ~ 9.78 through all depths in Lake Kivu
244 (Figure 5b). Based on the uncertainty of 1% attributed to the $^{20}\text{Ne}/^{22}\text{Ne}$ ratio, a systematic depletion of
245 $^{20}\text{Ne}/^{22}\text{Ne}$ down to 9.72 cannot be excluded, but seems very unlikely. And, even if outgassing was
246 responsible for the observed atmospheric noble gas depletion, we need a second process to explain the
247 observed enrichment of ^{40}Ar compared to ^{36}Ar .

248 4.1.2 Scenario 2: Inflow of noble gas depleted groundwater

249 In scenario 2, the atmospheric noble gas concentrations of inflowing deep hydrothermal groundwater
250 (Table 3) are assumed to be significantly below ASW. One mechanism which can lead to inflow of noble
251 gas depleted water is described in (15) for the Red Sea and in (30) for the Michigan basin. Adapted for
252 Lake Kivu, the mechanism works as follows: i) groundwater is heated up in the volcanically active subsoil
253 thus leading to a free gas/steam phase, ii) the noble gases preferentially partition into the gas/steam phase

254 and iii) gas and water phases are separated, and only the water phase, now depleted in noble gases, reaches
255 the lake. In Lake Kivu, the water temperature close to supposed hydrothermal groundwater inflows
256 exceeds that of the lake water by a few degrees (Table 1 in (3)), which suggests that indeed the
257 groundwater had been heated up before entering the lake. Other possible causes for noble gas depletion in
258 groundwater are sketched in (30), including gas exchange between groundwater and an initially noble gas
259 free oil phase. As heavier noble gases are more soluble in oil, this would explain why ³⁶Ar and Kr are
260 more depleted in Lake Kivu compared to Ne. Incidentally, oil prospection is indeed going on in the Lake
261 Kivu region (31).

262 4.1.3 Large past outgassing event

263 Scenario 3 assumes at least one large outgassing event to have happened in the past, which is supported by
264 observations in sediment cores (8,32,33). During such an event, not only large parts of the main gases CO₂
265 and CH₄ would leave the lake, but also most of the atmospheric noble gases would be stripped.
266 Subsequently, groundwater inflow and exchange with the atmosphere would slowly increase the noble gas
267 concentrations until they reach values close to ASW again after hundreds of years. Note that in this
268 scenario, in contrast to scenario 2, the hydrothermal groundwater sources are assumed to have noble gas
269 concentrations close to ASW.

270 We can do a plausibility check for this scenario by comparing the residence time of the deep water (i.e.
271 below ~265 m) to the time elapsed since the last supposed lake overturn. If one of these times is much
272 larger than the other, we can exclude scenario 3 because of either too slow or too fast flushing of the water
273 since the last overturn. However, both times are comparable and estimated to around 1000 years (see (2)
274 for residence time and (8) for time elapsed since lake overturn). Based on this, we can expect the deep
275 water to be completely replaced by hydrothermal groundwater within 1000 years. This means that there
276 was enough inflow of noble gas saturated groundwater to bring the deep lake water close to saturation
277 again. The reason why our observations differ from saturation could be explained by the absence of

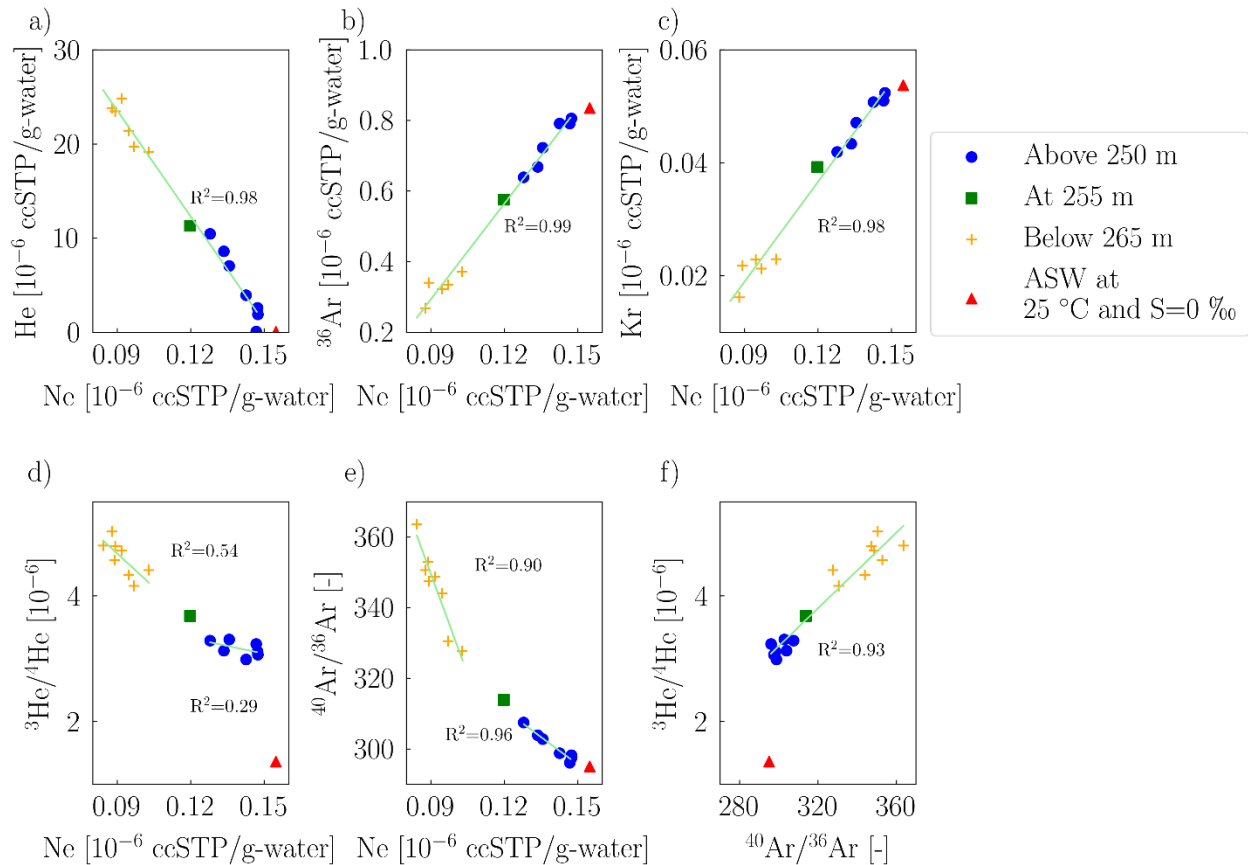
278 mixing processes in this assessment. Mixing may retain an unknown fraction of the depleted lake water in
279 the deep layers, thus keeping this scenario within the realms of possibility.

280 Yet, due to their high density (as suggested by (3)), the deep groundwater sources 4 - 6 (Table 3) should
281 stratify at the lake bottom. And since in scenario 3 (and also 1), we assume that these sources are close to
282 saturation in atmospheric noble gases, we would expect increasing atmospheric noble gas concentrations
283 with depth towards the lake bottom for these scenarios. This seems to be in contradiction to our data, as
284 we recorded constant or rather monotonously decreasing atmospheric noble gas concentrations with depth
285 below 265 m (Figure 3). Therefore, our data does not support the concept of the deep waters being refilled
286 with atmospheric noble gases from the deep groundwater sources as suggested in scenarios 1 and 3.

287 4.1.4 Most realistic scenario

288 Scenario 1, the large-scale continuous outgassing is not very likely to happen in Lake Kivu due to i) the
289 tendency of bubbles to redissolve at any depth and ii) the constant $^{20}\text{Ne}/^{22}\text{Ne}$ ratio, which suggests that
290 isotope fractionation is not taking place. Similarly, we can reject scenario 3 by the lack of increasing noble
291 gas concentrations towards the lake bottom. Therefore, we retain scenario 2, the inflow of atmospheric
292 noble gas depleted groundwater, as the most promising scenario for the observed depletions in the lake.
293 Furthermore, the almost perfect correlation between Ne, ^{36}Ar and Kr (Figure 6b and c) supports the view
294 that this one mechanism can explain the depletion of all the atmospheric noble gas species.

295 As explained, in scenario 2 a fraction of the atmospheric noble gases is lost to a gas/steam phase in the
296 subsoil. In principle, we would expect that a larger fraction of Ne is lost compared to the more soluble
297 ^{36}Ar and Kr, which would lead to a larger depletion of Ne in the lake. However, we actually observe a
298 larger depletion for ^{36}Ar and Kr and less depletion for Ne. Possible explanations for this observation
299 include the contact of the hydrothermal groundwater sources with a (noble gas free) oil phase rather than
300 steam (30) or the presence of large amounts of excess air (11).



301
 302 **Fig. 6. a) – c) Noble gas concentrations are plotted against Ne, along with a linear fit. We have $R^2 > 0.98$ for the correlation**
 303 **between He, ^{36}Ar , Kr and Ne. d)–e) The relationship between noble gas ratios $^3\text{He}/^4\text{He}$ and $^{40}\text{Ar}/^{36}\text{Ar}$ against Ne is**
 304 **explained using two linear fits with different slopes. f) $^3\text{He}/^4\text{He}$ is plotted against $^{40}\text{Ar}/^{36}\text{Ar}$. The red triangle shows air**
 305 **saturated water at $T = 25\text{ °C}$ and $S = 0\text{ ‰}$.**

306

307 **4.2 Inflow of magmatic ^3He , ^{40}Ar and CO_2**

308 The increasing $^3\text{He}/^4\text{He}$ and $^{40}\text{Ar}/^{36}\text{Ar}$ ratios with depth (Figure 5a and c) confirm the presence of

309 magmatic gases and/or fluids in Lake Kivu, as suggested by (13). These results are similar to reported

310 observations from Lakes Nyos and Monoun (19). Furthermore, the monotonous increase with depth of

311 these isotope ratios indicate that the main source has to be located close to the lake bottom (i.e. below the

312 maximum sampling depth of 440 m). For scenario 2 of section 4.1., this suggests that ascending magmatic

313 gases mix with groundwater in the subsoil, subsequently enter the lake and stratify at the lake bottom. The

314 linear relationship between Ne, $^3\text{He}/^4\text{He}$ and $^{40}\text{Ar}/^{36}\text{Ar}$ on Figures 6d) and e) below 265 m confirms this

315 link between atmospheric noble gas depletion and magmatic gases. However, the slope of this relationship

316 changes above 250 m. There, the inflow of a different kind of groundwater is supposed at ~250 – 255 m
317 and 135 – 180 m ((2,3) and Table 3). The hypothesis of inflow of groundwater admixed with magmatic
318 gases is also in line with the explanation of Nagao et al. (19) for enriched $^3\text{He}/^4\text{He}$ and $^{40}\text{Ar}/^{36}\text{Ar}$ ratios in
319 volcanic lakes Nyos and Monoun in Cameroon. The comparatively higher $^3\text{He}/^4\text{He}$ and $^{40}\text{Ar}/^{36}\text{Ar}$ values
320 found in these lakes (up to $\sim 8 \times 10^{-6}$ and ~ 550 respectively, compared to $\sim 5 \times 10^{-6}$ and ~ 365 in Lake Kivu)
321 can be readily explained by a higher fraction of magmatic gases in the respective mixture.

322 We can further use our isotope data to compute the $^3\text{He}/^{40}\text{Ar}^*$ ratio, where $^{40}\text{Ar}^*$ is the excess, non-
323 atmospheric ^{40}Ar , computed as $^{40}\text{Ar}^* = ^{36}\text{Ar} [(^{40}\text{Ar}/^{36}\text{Ar})_{\text{measured}} - (^{40}\text{Ar}/^{36}\text{Ar})_{\text{air}}]$. The $^3\text{He}/^{40}\text{Ar}^*$ values in
324 the deep water of Lake Kivu of $0.6 - 0.8 \times 10^{-5}$ (Table 2) are somewhat smaller than maximum values
325 found for the Nyiragongo crater fumaroles of around 1.1×10^{-5} (calculated from the data in (13)). In
326 addition, we can use the CO_2 measurements of M. Halbwachs and J.-C. Tochon (published in (2)) together
327 with our ^3He measurements to derive the $\text{CO}_2/^3\text{He}$ ratio (Table 2). We find values of $17 - 21 \times 10^9$ in the
328 Lake Kivu deep waters which agree very well with the Nyiragongo crater gas values of $\sim 20 \times 10^9$ found
329 by Tedesco et al. (13). The $\text{CO}_2/^3\text{He}$ ratios therefore confirm that the CO_2 in Lake Kivu is mostly of
330 volcanic origin.

331 4.3 Input of radiogenic ^4He and its link with atmospheric noble gas depletion

332 Figures 4 and 6a show that the He concentrations correlate very well with salinity and Ne concentrations
333 (and thus the concentrations of the other atmospheric noble gases ^{36}Ar and Kr). These correlations
334 strongly suggest that the He excess in Lake Kivu is governed by the same mechanism as these quantities,
335 i.e. by the hydrothermal groundwater inflows. However, the admixture of magmatic gases (previous
336 section) and the dilution by fresh water sources (Table 3) alone are not sufficient to explain the observed
337 He concentration and $^3\text{He}/^4\text{He}$ ratio profiles. Specifically, the He concentration in the (supposedly) ASW
338 saturated fresh groundwater sources is >2 orders of magnitude lower than in the deep water and therefore,
339 there is simply not enough ^4He to generate the observed $^3\text{He}/^4\text{He}$ profile. To show this, we use the total
340 hydrothermal and fresh discharges given in Table 3. In this situation, $\sim 4.55 \text{ m}^3/\text{s}$ of deep water with $2.4 \times$

341 10^{-6} ccSTP/g He and a $^3\text{He}/^4\text{He}$ ratio of 5.03×10^{-6} (Table 1) are diluted by ~ 37 m³/s with He = 3.8×10^{-8}
342 ccSTP/g and $^3\text{He}/^4\text{He} = 1.36 \times 10^{-6}$ (i.e. ASW, see Table 1). The resulting $^3\text{He}/^4\text{He}$ ratio at ~ 100 m depth is
343 only $\sim 1\%$ lower than at 410 m due to the large difference in total He concentration between the two
344 components. However, in our data we observe a change of the $^3\text{He}/^4\text{He}$ ratio from $\sim 5 \times 10^{-6}$ to $\sim 3 \times 10^{-6}$,
345 i.e. a decrease of 40%. To explain this large difference, we suggest the contribution of radiogenic ^4He
346 (with $^3\text{He}/^4\text{He}=10^{-8}$), produced in the rocks (11). We calculate that we need ~ 50 times more ^4He from
347 radiogenic production than from the ASW saturated groundwater sources to obtain the observed change
348 with depth of He concentration and $^3\text{He}/^4\text{He}$ ratio in Lake Kivu.

349 Moreover, the measured $^3\text{He}/^4\text{He}$ ratios in the deep waters of Lake Kivu are only around half of that in its
350 supposed source, i.e. the magmatic gases of the Nyiragongo volcano. The mixture of these magmatic
351 gases with ASW saturated groundwater cannot produce water with high He and $^3\text{He}/^4\text{He}$ values at the
352 same time. If the mixture involves enough groundwater to lower the $^3\text{He}/^4\text{He}$ ratio to around 50% of its
353 original value, the corresponding decrease in He concentration would be 98 %. Once again, the
354 contribution of both radiogenic and magmatic He is required to explain the observed He concentrations
355 and $^3\text{He}/^4\text{He}$ ratios.

356 Overall, we suggest that the observed He concentration and $^3\text{He}/^4\text{He}$ ratio profiles can be explained by a
357 combination of hydrothermal He inflow with $\sim 50\%$ He derived from magmatic gases and $\sim 50\%$ of
358 radiogenic ^4He (the effect of ASW saturation is negligible) and fresh groundwater inflow with $\sim 98\%$ He
359 from radiogenic ^4He and $\sim 2\%$ from ASW saturation.

360 **5 Conclusion**

361 We successfully analyzed noble gas concentrations in highly gas-rich Lake Kivu. The in-situ noble gas
362 sampling showed a remarkable depletion of atmospheric noble gases Ne, ^{36}Ar and Kr by about 45 to 70%
363 compared to ASW. In addition, magmatic noble gas isotopes ^{40}Ar and ^3He , as well as radiogenic ^4He are
364 enriched in the deep waters. The $^3\text{He}/\text{CO}_2$ ratio observed in the deep water is very similar to values found

365 for the Nyiragongo crater gas, supporting the idea that the CO₂ in Lake Kivu is indeed mostly of magmatic
366 origin.

367 We presented three possible mechanisms which could lead to the observed noble gas depletion. Scenario
368 1, the continuous stripping of noble gases in the lake by bubbles, is not supported by our ²⁰Ne/²²Ne and
369 ⁴⁰Ar/³⁶Ar profiles. There is no fractionation in the ²⁰Ne/²²Ne profile, which indicates that kinetic
370 fractionation during bubble formation did not occur. Scenario 3 consists of an initially atmospheric noble
371 gas free lake (after an overturn) and the gases are resupplied by hydrothermal sources. This scenario is
372 largely compatible with reported residence time and groundwater discharges. However, the salinity profile
373 suggests that the groundwater sources stratify at the lake bottom and thus we should observe the largest
374 concentrations of atmospheric noble gases close to the bottom. In contrast, our observations show the
375 lowest concentrations at the largest depths.

376 Scenario 2, the inflow of noble gas depleted groundwater, is best supported by our data. The arguments in
377 favor include positive temperature spikes (as observed by (3)) at supposed locations of groundwater
378 inflows and a very good correlation between atmospheric noble gases and He, indicating that the depletion
379 of atmospheric gases and the enrichment of He have a common origin. We also observe that Ne is less
380 depleted than the more soluble ³⁶Ar and Kr. To explain this, a considerable amount of excess air needed to
381 be trapped during original infiltration of the water, which later formed the hydrothermal sources (11).

382

383 **Acknowledgements**

384 We would like to thank Reto Britt, Michael Plüss, Ivo Beck, Maximilian Schmidt and the whole team
385 from LKMP (Lake Kivu Monitoring Programme) for help with field work. Augusta Umutoni and Ange
386 Mugisha from LKMP for help with the organization of the field campaigns. Andreas Raffainer and the
387 Eawag workshop for the development of the in-situ sampling mechanism. Edith Horstmann and
388 Alexandra Lightfoot for help with sample analysis.

389 Funding: This project was supported by the Swiss National Science Foundation (grant 200021_160114).

390

391 **References**

- 392 (1) Muvundja, F. A.; Wüest, A.; Isumbisha, M.; Kaningini, M. B.; Pasche, N.; Rinta, P.; Schmid, M.
393 (2014). Modelling Lake Kivu water level variations over the last seven decades. *Limnologica* 47,
394 21-33.
- 395 (2) Schmid, M.; Halbwegs, M.; Wehrli, B.; Wüest, A. (2005). Weak mixing in Lake Kivu: new
396 insights indicate increasing risk of uncontrolled gas eruption. *Geochemistry, Geophysics,*
397 *Geosystems*, 6(7), Q07009.
- 398 (3) Ross, K. A.; Gashugi, E.; Gafasi, A.; Wüest, A.; Schmid, M. (2015). Characterisation of the
399 subaquatic groundwater discharge that maintains the permanent stratification within Lake Kivu;
400 East Africa. *PloS one*, 10(3), e0121217.
- 401 (4) Pasche, N.; Dinkel, C.; Müller, B.; Schmid, M.; Wüest, A.; Wehrli, B. (2009). Physical and
402 biogeochemical limits to internal nutrient loading of meromictic Lake Kivu. *Limnology and*
403 *Oceanography*, 54(6), 1863-1873.
- 404 (5) Schoell, M.; Tietze, K.; Schoberth, S. M. (1988). Origin of methane in Lake Kivu (east-central
405 Africa). *Chemical Geology*, 71(1-3), 257-265.
- 406 (6) Pasche, N.; Schmid, M.; Vazquez, F.; Schubert, C. J.; Wüest, A.; Kessler, J. D.; Pack, M.A.;
407 Reeburgh W.S; Bürgmann, H. (2011). Methane sources and sinks in Lake Kivu. *Journal of*
408 *Geophysical Research: Biogeosciences*, 116(G3), G03006.
- 409 (7) Haberyan, K. A.; Hecky, R. E. (1987). The late Pleistocene and Holocene stratigraphy and
410 paleolimnology of Lakes Kivu and Tanganyika. *Palaeogeography, Palaeoclimatology,*
411 *Palaeoecology*, 61, 169-197.
- 412 (8) Ross, K. A.; Schmid, M.; Ogorka, S.; Muvundja, F. A.; Anselmetti, F. S. (2015). The history of
413 subaquatic volcanism recorded in the sediments of Lake Kivu; East Africa. *Journal of*
414 *paleolimnology*, 54(1), 137-152.
- 415 (9) Katsev, S.; Aaberg, A. A., Crowe, S. A.; Hecky, R. E. (2014). Recent warming of Lake Kivu.
416 *PloS one*, 9(10), e109084.

- 417 (10) Wüest, A.; Jarc, L.; Bürgmann, H.; Pasche, N.; Schmid, M. (2012), Methane formation and future
418 extraction in Lake Kivu, in *Lake Kivu* (pp. 165-180), Springer, Dordrecht.
- 419 (11) Kipfer, R.; Aeschbach-Hertig, W.; Peeters, F.; Stute, M. (2002). Noble gases in lakes and ground
420 waters. *Reviews in mineralogy and geochemistry*, 47(1), 615-700.
- 421 (12) Holzner, C. P.; McGinnis, D. F.; Schubert, C. J.; Kipfer, R.; Imboden, D. M. (2008). Noble gas
422 anomalies related to high-intensity methane gas seeps in the Black Sea. *Earth and Planetary
423 Science Letters*, 265(3-4), 396-409.
- 424 (13) Tedesco, D.; Tassi, F.; Vaselli, O.; Poreda, R. J.; Darrah, T.; Cuoco, E.; Yalire, M. M. (2010). Gas
425 isotopic signatures (He, C, and Ar) in the Lake Kivu region (western branch of the East African
426 rift system): Geodynamic and volcanological implications. *Journal of Geophysical Research:
427 Solid Earth*, 115, B01205.
- 428 (14) Beyerle, U.; Aeschbach-Hertig, W.; Imboden, D. M.; Baur, H.; Graf, T.; Kipfer, R. (2000). A
429 mass spectrometric system for the analysis of noble gases and tritium from water samples.
430 *Environmental Science & Technology*, 34(10), 2042-2050.
- 431 (15) Winckler, G.; Kipfer, R.; Aeschbach-Hertig, W.; Botz, R.; Schmidt, M.; Schuler, S.; Bayer, R.
432 (2000). Sub sea floor boiling of Red Sea Brines: New indication from noble gas data. *Geochimica
433 et Cosmochimica Acta*, 64(9), 1567-1575.
- 434 (16) Weiss, R. F. (1970). The solubility of nitrogen, oxygen and argon in water and seawater. *Deep
435 Sea Res.*, 17(4), 721-735.
- 436 (17) Weiss, R. F. (1971). Solubility of helium and neon in water and seawater. *Journal of Chemical &
437 Engineering Data*, 16(2), 235-241.
- 438 (18) Weiss, R. F.; Kyser, T. K. (1978). Solubility of krypton in water and sea water. *Journal of
439 Chemical and Engineering Data*, 23(1), 69-72.
- 440 (19) Nagao, K.; Kusakabe, M.; Yoshida, Y.; Tanyileke, G. (2010). Noble gases in Lakes Nyos and
441 Monoun, Cameroon. *Geochemical Journal*, 44(6), 519-543.

- 442 (20) Wüest, A.; Piepke, G.; Halfman, J. D. (1996), Combined effects of dissolved solids and
443 temperature on the density stratification of Lake Malawi, in *The Limnology, Climatology and*
444 *Paleoclimatology of the East African Lakes* (pp. 183–202), Gordon and Breach, New York.
- 445 (21) Kling, G. W.; Clark, M. A.; Compton H. R.; Devine, J. D.; Evans, W. C.; Humphrey, A. M.;
446 Koenigsberg, E. J.; Lockwood, J. P.; Tuttle, M. L.; Wagner, G. N. (1987), The 1986 Lake Nyos
447 gas disaster in Cameroon, West-Africa. *Science*, 236(4798), 169–175
- 448 (22) Sigurdsson, H.; Devine, J. D.; Tchoua, F. M.; Presser, T. S; Pringle, M. K. W.; Evans, W. C.
449 (1987), Origin of the lethal gas burst from Lake Monoun, Cameroun, *Journal of Volcanology and*
450 *Geothermal Research*, 31(1–2), 1–16.
- 451 (23) Walter, K. M.; Zimov, S. A.; Chanton, J. P.; Verbyla, D.; Chapin III, F. S. (2006). Methane
452 bubbling from Siberian thaw lakes as a positive feedback to climate warming. *Nature*, 443(7107),
453 71.
- 454 (24) McGinnis, D. F.; Greinert, J.; Artemov, Y.; Beaubien, S. E.; Wüest, A. (2006). Fate of rising
455 methane bubbles in stratified waters: How much methane reaches the atmosphere?. *Journal of*
456 *Geophysical Research: Oceans*, 111, C09007.
- 457 (25) Leifer, I.; Culling, D. (2010). Formation of seep bubble plumes in the Coal Oil Point seep field.
458 *Geo-Marine Letters*, 30(3-4), 339-353.
- 459 (26) Greinert, J.; McGinnis, D. F.; Naudts, L.; Linke, P.; De Batist, M. (2010). Atmospheric methane
460 flux from bubbling seeps: Spatially extrapolated quantification from a Black Sea shelf area.
461 *Journal of Geophysical Research: Oceans*, 115, C01002.
- 462 (27) Degens, E. T.; von Herzen, R. P.; Wong, H. K.; Deuser, W. G.; Jannasch, H. W. (1973). Lake
463 Kivu: structure, chemistry and biology of an East African rift lake. *Geologische Rundschau*,
464 62(1), 245-277.
- 465 (28) Brennwald, M. S.; Kipfer, R.; Imboden, D. M. (2005). Release of gas bubbles from lake sediment
466 traced by noble gas isotopes in the sediment pore water. *Earth and Planetary Science Letters*,
467 235(1-2), 31-44.

- 468 (29) Tyroller, L.; Brennwald, M. S.; Mächler, L.; Livingstone, D. M.; Kipfer, R. (2014). Fractionation
469 of Ne and Ar isotopes by molecular diffusion in water. *Geochimica et Cosmochimica Acta*, 136,
470 60-66.
- 471 (30) Ma, L., Castro, M. C., & Hall, C. M. (2009). Atmospheric noble gas signatures in deep Michigan
472 Basin brines as indicators of a past thermal event. *Earth and Planetary Science Letters*, 277(1-2),
473 137-147.
- 474 (31) Mugisha, I. R. (2018). British firm searches for oil in Rwanda. *The East African*, 27 February.
475 Available at: [https://www.theeastafrican.co.ke/rwanda/Business/British-firm-to-search-for-oil-in-](https://www.theeastafrican.co.ke/rwanda/Business/British-firm-to-search-for-oil-in-Rwanda/1433224-4322042-ibxqoz/index.html)
476 [Rwanda/1433224-4322042-ibxqoz/index.html](https://www.theeastafrican.co.ke/rwanda/Business/British-firm-to-search-for-oil-in-Rwanda/1433224-4322042-ibxqoz/index.html)
- 477 (32) Zhang, X., Scholz, C. A., Hecky, R. E., Wood, D. A., Zal, H. J., & Ebinger, C. J. (2014). Climatic
478 control of the late Quaternary turbidite sedimentology of Lake Kivu, East Africa: Implications for
479 deep mixing and geologic hazards. *Geology*, 42(9), 811-814.
- 480 (33) Votava, J. E.; Johnson, T. C.; Hecky, R. E. (2017). Holocene carbonate record of Lake Kivu
481 reflects the history of hydrothermal activity. *Proceedings of the National Academy of Sciences*,
482 114(2), 251-256.

483 **Declarations of interest:** none